Xray, ultraviolet, and synchrotron radiation excited innervalence photoelectron spectra of CH4

M. Carlsson Göthe, B. Wannberg, L. Karlsson, S. Svensson, P. Baltzer et al.

Additional information on J. Chem. Phys.

X-ray, ultraviolet, and synchrotron radiation excited inner-valence photoelectron spectra of CH$_4$

M. Carlsson Göthe, B. Wannberg, L. Karlsson, S. Svensson, and P. Baltzer

Department of Physics, Uppsala University, Box 530, S-75121 Uppsala, Sweden

F. T Chau

Department of Applied Biology and Chemical Technology, Hong Kong Polytechnic, Hung Hom, Kowloon, Hong Kong

M-Y Adam

LURE, Bat 209 D, Université Paris-Sud, F-91405 Orsay, France

The inner-valence electron states of the methane molecule have been studied by means of x-ray, synchrotron radiation, and UV-photoelectron spectroscopy. Five correlation satellites have been identified and a detailed study has been carried out of the $2a_1^{-1}$ single hole state. For this state a Franck–Condon analysis has been performed, suggesting an equilibrium bond distance of 1.279 Å. The vibrational lines have a Lorentzian shape and the linewidth increases gradually with the vibrational quantum number. This probably indicates a reduction of the lifetime of the vibrational states due to predissociation. A discussion of the potential curves related to the correlation satellites is included.

I. INTRODUCTION

The electron configuration of the methane molecule is $(1a_1)^2(2a_1)^2(1t_2)^6$, where $1a_1$ is the C 1s core orbital with a binding energy of 290.7 eV.[1] The $1t_2$ orbital has an average binding energy of about 14.5 eV[2-5] and is responsible for a large part of the chemical bonding in the molecule. The ionization leads to a triply degenerate state $(1t_2)$ (Ref. 5) $^2T_2$, which is unstable towards Jahn–Teller interaction. Thus, the 2.5 eV width at half-maximum (FWHM) of the photoelectron band is partly associated with the splitting of the final state into several components, which have different energies in the Franck–Condon region.

The Auger electron spectrum recorded for transitions to the $1t_2^{-2}$ final state shows a very broad structureless peak suggesting that the vertical double ionization energy (peak maximum) is 40.7 eV.[6] A very high value of 38.6 eV was obtained also in a direct double charge transfer (DCT) experiment[7] and in photoion–photoion coincidence (PIPICO) measurements a threshold energy of 35.0 eV was measured.[8] On the other hand, from stepwise charge stripping reactions (CH$_4$ → CH$_4^+$ → CH$_4^{2+}$) a much lower value of 30.6 eV[9] was found. An explanation of the difference between the high binding energy results in Refs. 6 and 7, obtained for more or less Franck–Condonlike transitions, and the low binding energy results from the charge stripping experiment was offered by large scale MCSCF and CI calculations,[10] which showed that the potential minimum of CH$_4^{2+}$ corresponds to a planar D_{4h} configuration with much lower energy than for tetrahedral geometries. The calculated double ionization energy for this configuration was found to be 32.2 ± 0.3 eV. Thus, the high energy observed in the Auger electron, double charge transfer, and PIPICO spectra should reflect the fact that the transitions in these experiments involve a strongly sloping region of the potential surface several eV above the potential minimum. The difference

of about 2 eV between the Auger and DCT energies can at least partly be explained by the fact that the equilibrium bond distance is smaller in the core hole state than in the neutral ground state.[1] The much lower double ionization energy of 30.6 eV obtained in the charge stripping experiment could be due to a transfer of internal energy in the stepwise double ionization process.

Much less attention has been paid to the properties of the singly charged inner-valence primary hole state $2a_1^{-1}$ and the correlation satellite states in this energy region. In order to obtain further information related to the inner-valence region we have therefore carried out a new study by means of photoelectron spectroscopy using HeII, monochromatized x-ray and synchrotron radiation for the excitation. This study has been accompanied by a Franck–Condon factor analysis to determine the equilibrium geometry of the $2a_1^{-1}$ state and to obtain information about the potential curves for the different correlation states in this region. These states are, in principle, the same as those reached in Auger transitions and are therefore characterized by substantial changes in geometry and symmetry as predicted in Ref. 10. They may also be influenced by the same dissociation processes.

II. EXPERIMENTAL DETAILS

The UV excited inner-valence photoelectron spectrum of methane was recorded using an electrostatic electron spectrometer described in detail elsewhere.[11] It is equipped with a hemispherical energy analyzer with a central radius of 144 mm. A microchannel plate (MCP) detector system is used for detection of the electrons. This device contains two microchannel plates, mounted in a chevron arrangement, followed by a phosphor screen which transforms the electron pulses into light pulses detected by a TV camera. The spectrum was excited by means of HeIIα radiation produced

by a microwave powered electron cyclotron resonance (ECR) discharge light source. The source has been designed to operate at very low gas pressures (≈ 50 mTorr) to produce narrow lines. It provides a very high intensity, both from neutral and ionized gas in the discharge, due to a high power density. The detailed design of the source and the characteristics of the radiation produced have been reported elsewhere.[12]

The x-ray excited photoelectron spectrum was recorded using monochromatized Al Kα radiation at 1487 eV. The electron spectrometer used in these studies has an energy analyzer of mean radius 360 mm and a detection system of the same kind as the uv instrument. Both the uv and x-ray excited spectra were induced by means of unpolarized radiation, and the photoelectrons were detected at 90° against the photon beam.

During the recording of the UV excited spectrum some of the helium gas from the discharge source leaked into the gas cell. Thus, the spectrum contained a narrow line at 24.587 eV due to ionization of helium. This line was used as a reference for calibration of the uv excited spectrum. These energies were in turn used to calibrate the x-ray excited spectrum.

The synchrotron radiation excited spectrum was obtained at LURE using a 127° analyzer working in a constant pass energy mode. The excitation energy was set at 65 eV. To carry out angular resolved measurements the analyzer is rotable 180° around the incident polarized radiation. The present studies were performed at the angle 90°. The detailed experimental procedure is described elsewhere.[13]

III. METHODS OF CALCULATIONS

Calculations have been carried out on the totally symmetric vibrational mode $\nu_1(a_1)$ for the $X\,^1A_1$ neutral ground state[14-16] and in the $A\,^2A_1$ ionic state.[2,4] In tetrahedral XH$_4$ molecules, the internal coordinate S_1 for the a_1 mode is given by

$$S_1(a_1) = (\Delta r_1 + \Delta r_2 + \Delta r_3 + \Delta r_4)/2$$

with r_i being the X–H$_i$ internuclear distance. The inverse kinetic energy matrices $G_s(a_1)$ required in the normal coordinate analyses were setup by the standard method.[17]

To deduce the change in bond length upon the $X\,^1A_1 \rightarrow A\,^2A_1$ ionization process, the iterative Franck–Condon analysis procedure[18] was applied to the second photoelectron band. The shifts in normal coordinates thus obtained were converted to the changes in bond length with the use of the $L_s(a_1)$ matrices obtained in the force constant calculations.

IV. RESULTS AND DISCUSSION

A. The x-ray and synchrotron radiation photoelectron spectra

The x-ray excited ($h\nu = 1487$ eV) photoelectron spectrum of methane has been recorded in an energy region up to 60 eV. This is shown in Fig. 1. The energies, relative intensities, and widths (FWHM) of the observed lines or structures are collected in Table I. These values were obtained by fitting
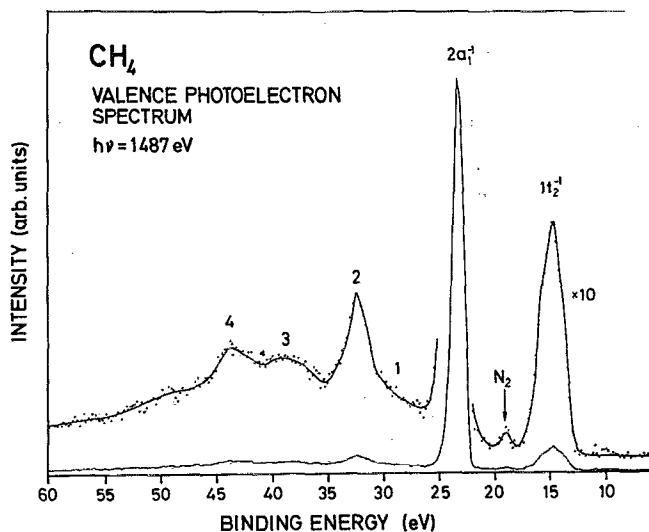

FIG. 1. The valence photoelectron spectrum of methane excited by means of monochromatized Al Kα radiation at 1487 eV. Numbers 1–4 refer to correlation satellite states. Another weak state is inferred at ~48 eV but is not indicated by a figure.

Gaussian lines to the observed structures and varying the peak positions, heights, and widths until the best fit was obtained. At the high kinetic energy in this experiment the transmission of the spectrometer can be regarded as constant over the studied energy interval. Since the photoelectron intensity of the satellites is low and the lines in the spectra are very broad the uncertainties in the data referring to these states are large, which is also reflected by the scattering of the energy values in the table. The energies given are average values from the x-ray and synchrotron radiation excited spectra.

The transitions to the $1t_2^{-1}$ and $2a_1^{-1}$ single hole states are readily observed at approximately 14 and 23 eV, respectively. The $2a_1$ orbital has a dominating $C\,2s$ character, which is reflected in the x-ray excited spectrum by the high intensity of the photoelectron line (cf. Fig. 1 and Table II). At higher binding energies additional satellite structure is observed. The most intense peak at 32.1 eV is accompanied by a weaker, but much broader (cf. Table I) feature centered at approximately 29.2 eV. At about 38.5 and 43.3 eV one very broad and one narrower structure, respectively, are observed. Above peak No. 4 an intense continuum is seen with a broad resonant structure centered at about 48 eV. In Fig. 1 and Table I we have labeled all satellite structures 1, 2, 3, and 4 in order of increasing binding energy.

The synchrotron radiation inner-valence photoelectron spectrum taken at 65 eV excitation energy is shown in Fig. 2. This spectrum is very similar to the present x-ray excited spectrum.

Structures 1 and 2 probably correspond to the structures observed at 28 and 31 eV in the ($e,2e$) spectrum[19] since they are similar in energy. The ($e,2e$) spectrum was recorded at an incident electron energy of 3.5 keV which was considered to be sufficiently high for the ($e,2e$) spectrum to simulate the photoelectron spectrum. Nevertheless, the line shapes are quite different from the photoelectron spectra

TABLE I. The electron binding energies, relative intensities and linewidths in the inner-valence region of the photoelectron spectrum of the CH$_4$ molecule measured with XPS and SRPS. The binding energies refer to the point of maximum intensity of the band and the relative intensities correspond to the peak area obtained by a curve fitting. The UPS linewidth was obtained from Fig. 4 and is included for comparison.

Line	Electron binding energy (eV)	Relative intensity[a]			Linewidth (FWHM)		
		XPS 1487 (eV)	SRPS 65 (eV)	UPS 40.8 (eV)	XPS 1487 (eV)	SRPS 65 (eV)	
$1t_2^{-1}$	14.5	0.10	$\cdots$	$\cdots$	1.3	$\cdots$	
$2a_1^{-1}$	23.0	1.00	1.00	0.90	0.9	0.9	
1	29.2	0.09	0.16		≈ 4	≈ 4	
2	32.1	0.04	0.06		1.3	1.4	
3	38.5	0.15	0.08		≈ 5	≈ 4	
4	43.3	0.10	0.05		1.7	1.4	

[a] Relative to the $2a_1^{-1}$ main line.

obtained both at low and high excitation energies. Especially structure 1 is much broader in the photoelectron spectra than in the (e,2e) spectrum.

The strongest satellite lines in x-ray excited photoelectron spectra are usually produced by transitions which involve unoccupied valence orbitals. In the case of methane there are two such orbitals, $2t_2$ and $3a_1$, the antibonding counterparts to the occupied orbitals of the same symmetry. The observed satellite structure is thus expected to primarily reflect excitations involving these orbitals. The strongest satellite intensity is expected for states that interact with the $2a_1$ $^1{}^2A_1$ single hole state, which has a large intensity in the x-ray excited photoelectron spectrum due to the high cross section for atomic C 2s orbitals. In the many-electron calculations by Cederbaum et al.[20] two CI states appeared at approximately 31 and 35 eV. These were associated with do-

minating $1t_2^{-2}2t_2$ and $1t_2^{-2}3a_1$ configurations and the intensity of the transitions was explained by a mixing of the $^2A_1$ component of the state manifold with the $2a_1^{-1}\,^2A_1$ single hole state. Disregarding an absolute energy shift of about 2–3 eV these energies fit with structures 1 and 2 of our spectra. The large widths of the structures (cf. Table I) are expected since the transitions involve strongly bonding and antibonding orbitals. In a recent study of excitation energies in neutral molecules by means of a specially parameterized complete neglect of differential overlap (CNDO) program[21] the $1t_2 \rightarrow 2t_2$ and $1t_2 \rightarrow 3a_1$ energies were found to be approximately 12 eV and 16 eV, respectively. If these energies are added to the energy 14 eV of the $1t_2^{-1}$ primary hole state we obtain 26 and 30 eV, respectively, for the $1t_2^{-2}2t_2$ and $1t_2^{-2}3a_1$ configurations. This is in reasonable agreement with the energies of lines 1 and 2, considering the fact

TABLE II. Vibrational energies, intensities and linewidths of the $2a_1$ ^1A $^2A_1$ photoelectron band of the methane molecule. The data were obtained from a curve fitting to the experimental spectrum. Lorentzian lines were used except for the first two peaks which were fitted by a weighted sum of a Lorentzian and a Gaussian. The weight factors are given in the table. A straight line background was subtracted.[a] The very weak lines 8–14 may be due to inelastic scattering of photoelectrons (see the text).

Line No.	Energy (eV)	Vibrational quantum number	Vibrational energy (eV)	Peak area	Linewidth (FWHM) (meV)[b]	Percentage of Gaussian function
1	22.411	0	0	0.4	70	30
2	22.680	1	0.269	0.9	100	10
3	22.941	2	0.530	1.0	130	0
4	23.199	3	0.788	0.8	150	0
5	23.454	4	1.043	0.5	160	0
6	23.69	5	1.28	0.2	180	0
7	23.94	6	1.53	0.1	200	0
8	24.18	7	1.77	0.03	≈ 200	0
9	24.45	8	2.01			
10	24.775					
11	25.012					
12	25.287					
13	25.525					
14	25.757					

[a] The linear background subtracted was obtained from the background intensities observed on the far right- and left-hand sides of the spectrum.
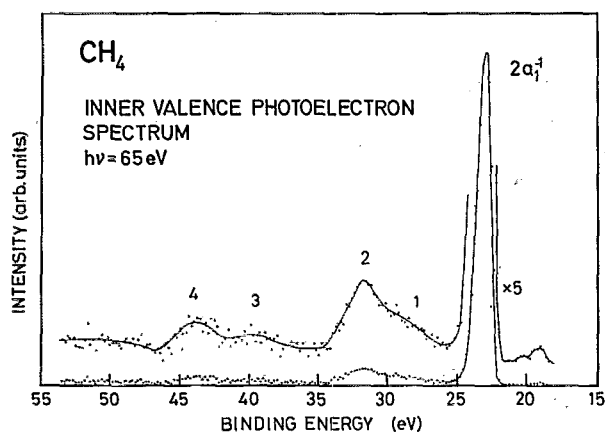[b] The error is estimated to be 10% of the FWHM.

FIG. 2. The valence photoelectron spectrum of methane excited by synchrotron radiation at 65 eV. Numbers 1–4 as in Fig. 1.

that these calculations did not take the $2a_1$ hole into account. Moreover, the width of line 1 is ≈ 3 eV which is much larger than the ~ 0.9 eV width of line 2. Since both of the lines are well below the threshold for double ionization the linewidth is determined by Jahn–Teller broadening and of the slope of the final state potential curves in the Franck–Condon region. The $2t_2$ orbital is more antibonding than the $3a_1$ orbital. The Jahn–Teller splitting of a strongly antibonding state is expected to be larger than for a less antibonding state. This obviously supports the assignment of lines 1 and 2 made above.

It is interesting to note that, although the uncertainties are large, the ratio of the intensity of structure 1 to structure 2 seems to be lower in the x-ray excited than in the synchrotron radiation excited spectrum. Differences in the β values between the two components may explain the difference in the relative intensity for the two excitations, since the spectra were not recorded at the magic angle. Measurements of β values have not yet been performed for the satellites. However, the β value for photoionization from the $2a_1$ orbital is high, increasing from about 1 in the low energy limit and approaching 2 in the high energy limit,[22,23] the value which is also expected for the $2s$ ionization from the neon atom. Such a similarity in the photoionization of CH$_4$ and Ne has been reported previously in Ref. 24, where the β value for ionization from the $1t_2$ orbital of CH$_4$ was shown to be similar to that for the $2p$ orbital of Ne. These values are generally lower than those of the $2s$ and $2a_1$ ionization. Differences in the composition of the correlation states may thus lead to differences in the photoelectron intensities. Since the behavior in the high energy limit is not known for the $2p$ and $1t_2$ orbitals it is not clear if such differences may lead to variations in the photoelectron intensities with the photon energy.

The large structures 3 and 4 observed at about 38.5 and 43.3 eV, respectively (cf. Table I), are both lying above the double ionization threshold in the Franck–Condon region of the neutral ground state at 35 eV.[8] They may therefore probably be associated with resonances in the double ionization continuum that can be seen as an increased intensity at high binding energies in Fig. 1. Due to their high energy, these

transitions could be due to excitations accompanying the $2a_1^{-1}$ primary hole. Two such transitions are allowed without the inclusion of vibronic coupling, leading to the final state configurations $2a_1^{-1} 1t_2^{-1} 2t_2$ and $2a_1^{-2} 3a_1$. Using the calculated excitation energy of 12 eV[21] for the neutral molecule, the first transition is expected to appear at binding energies higher than 35–36 eV, since the effect of the $2a_1^{-1}$ hole must be taken into account. This transition could thus correspond to structure 3. If we consequently associate structure 4 with a leading final state configuration $2a_1^{-2} 3a_1$, we obtain the $2a_1^1 \rightarrow 3a_1^1$ excitation energy above the $2a_1^{-1}$ primary hole state to be approximately $43.5-23 \approx 20$ eV. However, multiplet splitting could also explain both structures as originating from the same orbital shakeup process. This assignment is also supported by a consideration of the linewidths in Fig. 1. Line 3, associated with a $2t_2$ excitation, is very broad ($\approx 3-4$ eV) whereas line 4, associated with a $3a_1$ excitation, is relatively narrow with a width of ~ 1 eV. However, since lines 3 and 4 lie in the double ionization continuum also coupling of the discrete singly and doubly ionized continuum channels contribute to the linewidths. The extremely broad structure at about 48 eV is probably caused by such a resonance mechanism.

B. The UV excited photoelectron spectrum

Photoionisation out of the $2a_1$ orbital is possible using HeIIα radiation and the photoelectron band is observed at about 23 eV (cf. Fig. 3). The band displays a vibrational progression in the v_1 (a_1) mode, which is the only mode that is expected to be strongly excited in a nondegenerate electronic state. This progression has been observed also in previous studies[2,4,25] although not to as high vibrational quantum numbers as in the present investigation. The first peak corresponding to the adiabatic (0–0) transition is observed at 22.41 ± 0.01 eV. The 0–1 vibrational spacing is approximately 270 meV. This is much smaller than the corresponding neutral ground state vibrational spacing of 361 meV,
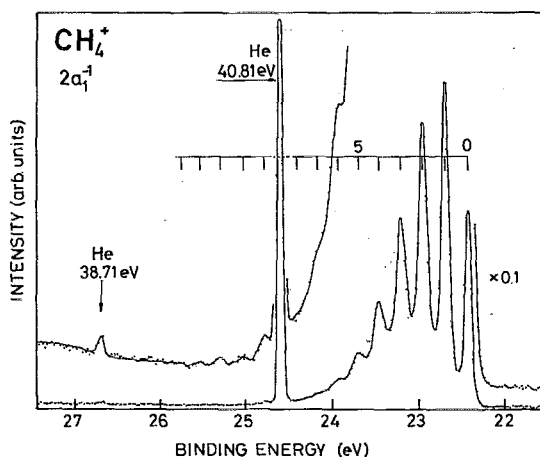

FIG. 3. The $2a_1^{-1}$ photoelectron band excited by means of HeIIα radiation at 40.8 eV. A vibrational progression in the v_1 (a_1) mode is observed. Ionization of He leaking into the gas cell from the uv source gives rise to the line at 24.587 eV. The weak lines indicated by bars on the high energy side of the He line may be due to inelastic scattering of photoelectrons (see the text).

suggesting that the chemical bonding is much weakened upon the removal of $2a_1$ the electron.

The vibrational spacings decrease towards higher quantum numbers, which gives an indication of the anharmonicity of the potential curve. We have tentatively fitted a Morse potential function to these data and thus obtained a dissociation energy of 4.70 eV along the totally symmetric q_1 normal coordinate. However, as will be discussed below, this value is much lower than the value determined from thermochemical and atomic data.

The equilibrium bond distance of the ionic state is obtained from a Franck–Condon analysis based on the relative intensities of the vibrational peaks, as described below. However, these intensities are not easily determined from the spectrum since the peaks are not fully resolved and, in addition, the line width is observed to increase with increasing quantum numbers. In order to analyse the band in further detail we have therefore fitted a series of model functions to the observed peaks. In this procedure the peak height and full width at half-maximum of the model functions were varied. The best result is shown along with the experimental spectrum in Fig. 4 and Table II. It was obtained using Lorentzians for all peaks except the first two, for which weighted sums of a Lorentzian and a Gaussian with equal line widths (approximate Voigt functions) were used. The weight factors of the latter are given in Table II together with the other parameters. Before the fitting was made, a straight line background, slightly sloping, was subtracted.

Since the widths of the lines increase successively towards higher vibrational quantum numbers it may be appropriate to use the areas in order to represent the relative intensities, instead of the peak heights which are often used. The maximum intensity is then obtained for the $v = 2$ level instead of $v = 1$, which exhibits the highest peak. This also implies a larger change in the C–H bond distance. Table II presents the areas of the peaks used in the Franck–Condon analysis for methane.

As can be seen from Fig. 4, the fitting of the model functions is good except in a range between the first two peaks, where the experimental intensity is not fully accounted for. The discrepancy appears with a maximum intensity at about 104 meV above the $v = 0$ peak. This could suggest a very weak excitation of a single quantum of the v_4 (t_2) mode or of the v_2 (e) mode. Higher components of a vibrational progression would hardly be seen due to the larger line widths in this region. The energy of the v_4 vibration in the neutral ground state is 162 meV and of the v_2 mode 189 meV. Excitations of this kind require a vibronic interaction with an electronically degenerate state of either $^2T_2$ symmetry or ^2E symmetry present in this energy range. Such states would arise from the two holes–one particle electron configurations $1t_2^{-2} 2t_2$ and $1t_2^{-2} 3a_1$. In CI calculations of the potential energy curves it has been shown that in the range of the $2a_1^{-1}$ state repulsive states of $^2A_1$ symmetry appear in the Jahn–Teller distorted systems both for C_{2v} and C_{3v} symmetry.[26] These repulsive states could be responsible for a predissociation of the $2a_1^{-1}$ single hole state (cf. also Sec. IV D).

Additional weak structures can be seen in the experimental spectrum on the high binding energy side of the He line at 24.587 eV (cf. Fig. 3). Five clearly discernible lines are indicated by bars in the figure and the energies are given in Table II. The average spacing between the peaks is about 240 meV. These peaks could be due to inelastic scattering of the photoelectrons in the gas cell leading to vibrational excitations of neutral methane molecules. The spacing between the He line and the first peak at 24.775 eV is 188 meV which fits exactly to the energy of the v_2 (e) mode in the neutral ground state.[14]

C. Franck–Condon factors

Removal of one electron from the $2a_1$ orbital will weaken the X–H bond appreciably, resulting in a large decrease in the energy of the symmetric stretching mode v_1 as well as in the corresponding force constants. In Table III, the force constants $F_s'(a_1)$ of methane, obtained in the present calculations, are given. The bond lengths derived for the ion together with that of the neutral molecule[27] are listed in Table
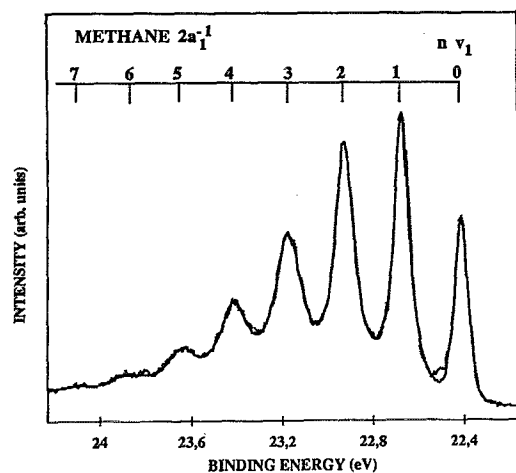

FIG. 4. A fitting of model functions to the spectrum of Fig. 3 using the parameters given in Table II. The fitted curve is given in black and the experimental curve in gray.

TABLE III. Molecular properties of the $X\,^1A_1$ neutral ground state and in the $A\,^2A_1$ ionic state of methane.

$X\,^1A_1$ state		
v_1 (cm^{-1})	2916.5^b	
$F_s(a_1)$ (md/Å)	5.050	
r_{CH} (Å)	1.0940^b	
$A\,^2A_1$ state		
v_1 (cm^{-1})	2030(10)^a	
$F_s'(a_1)$ (md/Å)	2.44(0.03)	
Δr_{CH} (Å)^c	0.185(0.004)	[$\rightarrow r_{CH}' = 1.279(0.004)$ Å]
E_B(ad.) (eV)	22.41	

^{a} Numbers within parentheses are estimated errors for the corresponding quantities.
^{b} Reference 14.
^{c} In Ref. 28 a value of 0.11 Å was reported for Δr_{CH}.

III. As can be seen, there is a considerable increase in bond length accompanying the $X\,^1A_1 \to A\,^2A_1$ ionization process. It should be mentioned that the relative intensities used in the Franck–Condon analysis were taken as the peak areas. No correction needs to be made for the differences in the kinetic energy, since the spectrometer transmission can be regarded as constant over the bandwidth.

D. Discussion of potential curves

The neutral ground state potential curve corresponding to the symmetric stretching normal coordinate can be estimated using the energy required to form a C + 4H complex. Using thermochemical data of Ref. 29 a dissociation energy of 17.0 eV is obtained for the symmetric stretch vibrational mode. The potential curve of the $2a_1^{-1}$ cationic state followed by assuming sustained symmetric stretch vibrations leads to the formation of the $C^+(2s^{-1}) + 4H$ complex. This requires a total energy of $17.0 + 11.27 + 5.33 = 33.6$ eV above the neutral molecular ground state using an energy of 11.27 eV for the first ionization potential of the carbon atom, corresponding to the formation of $C^+(2p^{-1})$ and a $C^+(2p^{-1}) \to C^+(2s^{-1})$ excitation energy of 5.33 eV.[30] A dissociation energy of $33.6 - 22.4 = 11.2$ eV is thus obtained for the symmetric stretch vibrational mode in this electronic state. The formation energy of the $C^+(2s^{-1}) + 4H$ complex obtained from a Morse potential curve, fitted to the observed vibrational spacings, is only 27.2 eV, which is more than 5 eV lower than 33.6 eV. Although the Morse potential does not, in general, provide accurate dissociation energies this very large difference may suggest that the shape of the potential curve is strongly influenced by a crossing with a repulsive state curve.

Some information about the potential curves of the correlation satellite states is obtained from the line shapes. The most intense peak at 32.1 eV (line 2 in Figs. 1 and 2), is fairly symmetric, suggesting that the Franck–Condon region falls on an essentially straight part of the potential curve. From the width of the line the slope can be estimated to be $\geqslant 15$ eV/Å. An even larger slope is found for line 1. The width of ~ 3 eV in this case indicates an enormous slope of ~ 50 eV/Å. These two structures probably correspond to two repulsive states of $^2A_1$ and ^2E symmetry predicted in Ref. 26. Also the difference of the slopes of the respective potential curves may be inferred from Fig. 8 in this reference. In the same work another even lower potential curve associated to $^2A_1$ symmetry is also predicted. In the XPS spectrum, taken at 1487 eV excitation energy with a high signal-to-background ratio, it is also seen that the intensity between the $2a_1^{-1}$ and $1t_2^{-1}$ lines is increased compared to the straight background which is observed on the right-hand side of the $1t_2^{-1}$ line. The small N₂ contribution cannot explain this increase. Therefore, the potential curve of the calculated state with $^2A_1$ symmetry, leading to dissociation in C_{2v} symmetry,[26] could be responsible for a predissociation of the $2a_1^{-1}$ state.

The strong coupling to the dissociation continuum has previously been shown in a photodissociative ionization study of CH₄ reported in Refs. 31 and 32. At the $2a_1^{-1}$

threshold, H^+ and CH^+ ions start to appear and there is also an increase in the CH_2^+ production. CH_3^+ which has several dissociation limits below 29.2 eV (cf. ionization energies in Ref. 33) is either not formed in predissociation of the $2a_1^{-1}$ state or is subject to further decay processes.

In the range of the present study five dissociation limits above the ionization threshold for the $2a_1$ orbital, leading to H^+ ions, have been observed by dissociative electroionization.[34] The energies of these are 26.3, 26.9, 29.4, 32.7, and 35.7 eV and it was concluded that these energies probably correspond to dissociation channels opened by predissociation of excited states of CH_4^+. All these energies are in the range of the observed satellite structure in the present x-ray and synchrotron radiation excited photoelectron spectra and at energies which roughly seem to correspond to onsets of the photoelectron bands. As suggested above, the final states of the photoelectron transitions up to about 32 eV belong to the $1t_2^{-2}\,3a_1$ and $1t_2^{-2}\,2t_2$ Jahn–Teller split manifolds, which agrees with the calculations in Ref. 26. Similarly, the higher energies could correspond to ionization processes connected to the other configurations discussed above. These states are embedded in the double ionization continuum. The first onset of CH_4^{2+} production was observed at 35.0 eV, with a vertical energy in the transition of 37.15 eV, and a second onset at 38.5 eV using PIPICO.[8] A more detailed ultraviolet photoemission spectroscopy (UPS) study using monochromatized Heɪɪα radiation, and an extended angular resolved study using synchrotron radiation would help to give more information on the band shapes which would enable more detailed interpretations.

ACKNOWLEDGMENTS

[1] L. Asplund, U. Gelius, S. Hedman, K. Siegbahn, and P. E. M. Siegbahn, Uppsala University, Institute of Physics Report, UUIP-1085, 1983.

[2] C. R. Brundle, M. B. Robin, and H. Basch, J. Chem. Phys. **53**, 2196 (1970).

[3] J. W. Rabalais, T. Bergmark, L. O. Werme, L. Karlsson, and K. Siegbahn, Phys. Scr. **3**, 13 (1971).

[4] A. W. Potts and W. C. Price, Proc. R. Soc. London, Ser. A **326**, 165 (1972).

[5] G. Bieri and L. Åsbrink, J. Electron Spectrosc. **20**, 149 (1980).

[6] R. Spohr, T. Bergmark, N. Magnusson, L. O. Werme, C. Nordling, and K. Siegbahn, Phys. Scr. **2**, 31 (1970).

[7] P. G. Fournier, J. Fournier, F. Salama, P. J. Richardson, and J. H. D. Eland, J. Chem. Phys. **83**, 241 (1985).

[8] G. Dujardin, D. Winkoun, and S. Leach, Phys. Rev. A **31**, 3027 (1985).

[9] T. Ast, C. J. Porter, C. J. Proctor, and J. H. Beynon, Chem. Phys. Lett. **78**, 439 (1981).

[10] P. E. M. Siegbahn, Chem. Phys. **66**, 443 (1982).

[11] P. Baltzer, B. Wannberg, and M. Carlsson, Uppsala University, Institute of Physics Report, UUIP-1182, 1989.

[12] P. Baltzer and L. Karlsson, Uppsala University, Institute of Physics Report, UUIP-1211, 1989.

[13] P. Morin, M-Y Adam, I. Nenner, J. Delwiche, M. J. Hubin-Franskin, and P. Lablanquie, Nucl. Instrum. Methods **208**, 761 (1983).

[14] G. Herzberg, *Electronic Spectra and Electronic Structure of Polyatomic Molecules* (Van Nostrand Reinhold, New York, 1966).

[15] T. Schimanouchi, *Tables of Molecular Vibrational Frequencies*, NSRDS-NBS 39 (National Bureau of Standards, Washington, D.C., 1972).

[16] L. May and C. R. Dillard, J. Chem. Phys. **34**, 694 (1961).

[17] E. B. Wilson Jr., J. C. Decius, and P. C. Cross, *Molecular Vibrations* (McGraw–Hill, New York, 1955).

[18] F. T. Chau, J. Electron Spectrosc. **48**, 389 (1989).

[19] M. J. van der Wiel, W. Stoll, A. Hamnett, and C. E. Brion, Chem. Phys. Lett. **37**, 240 (1976).

[20] L. S. Cederbaum, W. Domcke, J. Schirmer, W. von Niessen, G. H. F. Diercksen, and W. P. Kraemer, J. Chem. Phys. **69**, 1591 (1978).

[21] E. Lindholm, L. Åsbrink, S. Ljunggren, and J. Li (to be published).

[22] M. Y. Adam, C. Cauletti, M. N. Piancastelli, and A. Svensson, J. Electron Spectrosc. **50**, 219 (1990).

[23] M. Rosi, A. Sgamellotti, F. Tarantelli, V. A. Andreev, M. M. Gofman, and V. I. Nefedov, J. Electron Spectrosc. **41**, 439 (1986).

[24] G. V. Marr and R. M. Holmes, J. Phys. B **13**, 939 (1980).

[25] G. Bieri and L. Åsbrink, J. Electron Spectrosc. **20**, 149 (1980).

[26] E. F. van Dishoeck, W. J. van der Hart, and M. van Hemert, Chem. Phys. **50**, 45 (1980).

[27] *Table of Interatomic Distances and Configuration in Molecules*, edited by L. E. Sutton (Chemical Society, London, 1965).

[28] W. Meyer, J. Chem. Phys. **58**, 1017 (1973).

[29] S. G. Lias, J. E. Bartmess, J. F. Liebman, J. L. Holmes, R. D. Levin, and W. G. Mallard, J. Phys. Chem. Ref. Data **17**, Suppl. 1 (1988).

[30] C. E. Moore, Natl. Bur. Stand. (U.S.), Circ. **467** (1949).

[31] P. L. Kronebusch and J. Berkowitz, Int. J. Mass Spectrom. Ion Phys. **22**, 283 (1976).

[32] J. A. R. Samson, G. N. Haddad, T. Masuoka, P. N. Pareek, and D. A. L. Kilcoyne, J. Chem. Phys. **90**, 6925 (1989).

[33] J. M. Dyke, N. B. H. Jonathan, E. Lee, and A. Morris, J. Chem. Soc. Faraday Trans. 2 **72**, 1385 (1976).

[34] R. Locht and J. Momigny, Chem. Phys. **49**, 173 (1979).